

# Absence of reflectivity of the phonon-polariton at the SiC surface from the metal mask edge

V.S. Ivchenko, D.V. Kazantsev,\* V.A. Ievleva, D.A. Matienko, and A.Yu. Kuntsevich  
*P.N. Lebedev Physical Institute of the Russian Academy of Sciences, 119991, Moscow, Russia*

E.A. Kazantseva  
*Moscow Technological University, Moscow, Russia 119454*  
 (Dated: June 25, 2025)

Surface phonon polariton (SPhP) waves are excited at the silicon carbide (*SiC*) surface under irradiation of light close to the lattice resonance frequency. Metal mask at the surface blocks irradiation of certain areas and thus allows tuning standing or propagating wave pattern and, thus, open opportunities for surface polariton optic devices. In this study we show by means of scanning near-field microscopy that the edge of such a mask reflects SPhP waves negligibly. This condition differs dramatically from numerous recent observations of polariton reflections in 2D materials and makes the metallized *SiC* platform advantageous in a sense of capability to calculate wavefield using a simple Green function-based approach.

PACS numbers: 07.79.Fc, 68.37.Ps, 07.60.-j, 87.64.Je, 61.46.+w, 85.30.De, 68.65.Pq

**Introduction.** Surface phonon polariton (SPhP) waves could be excited by external irradiation at the surfaces of polar crystals and are therefore of great interest for on-chip surface optic applications [1]. SPhPs emerge if the frequency is close to the optical phonon frequency  $\omega_T$ , i.e., mechanical resonance of the lattice, where local dielectric permittivity reaches several hundreds [2, 3]. A

convenient and commonly accepted description of near-surface electromagnetic wave propagation is a simultaneous solution of the Maxwell equations for electromagnetic fields and the Newton equations for lattice atoms [4–7].

This model leads to the same equation as for the plasma of itinerant electrons in metals. Numerically, however, plasmon resonances in metals lie in the visible or UV spectral range owing to small electron mass, while SPhPs are located in the middle and far IR spectral range. For example, in *SiC* the resonance occurs at  $\nu_T(\text{SiC}) = 795 \text{ cm}^{-1}$ . The necessity to use dedicated IR lasers and photodetectors made surface phonon-polariton phenomena much less studied than plasmon-polaritons.

Similarly to surface plasmons, the SPhP waves are located in a thin layer close to the interface and could propagate in a lateral direction without much damping. It was previously demonstrated by scanning near-field optical microscopy (SNOM) methods that phonon polariton fields are influenced by patterns made of metal (usually gold) films or dielectric. Indeed, the field of incident wave does not reach the *SiC* surface under metal, (see Fig.1) while the dielectric film changes substantially the media interface boundary conditions. Depending on the design of the mask, various surface wave patterns are formed, including edge-launched waves [8, 9], resonators [10], single metal spot scatterers [11], concave mirrors [12], and diffraction gratings[13].

In recent years a great deal of interest arose to the surface IR plasmon or phonon-polariton electromagnetic waves in 2D materials, thin films, and heterostructures [10, 14–16]. SNOM studies in these papers reveal experimental observations of numerous phenomena related to the scattering or reflection of the surface waves at the boundaries of the mesa-defined elements or flakes. In particular, interference of the wave at the tip near the boundary with the reflected surface waves produces typical oscillations - a direct proof of the surface waves. For the surface of a bulk *SiC*, the tip plays a negligible role

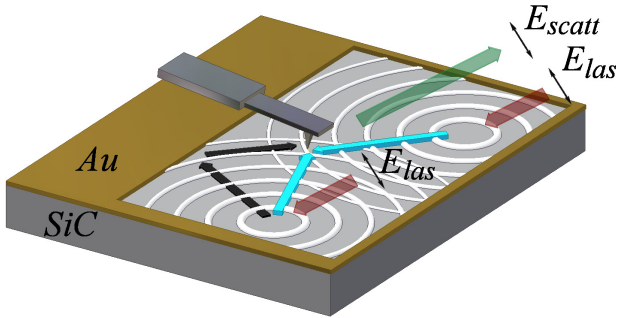


FIG. 1: Excitation of phonon-polariton waves on an open *SiC* surface by external irradiation. A phenomenon model assumes the use of the Green's function. Laser (transparent red arrows) light with constant amplitude  $E_{las}$  affects all points of the *SiC* surface not covered by the *Au* mask and generates concentrically diverging waves from them. These waves sum up at the point of the tip location, having arrived at it along the straight trajectories, indicated by light arrows. Under the action of the local field, the tip scatters a wave (transparent green arrow) with an amplitude  $E_{scatt}$  back into the instrument.  $E_{scatt}$  value is proportional to the total field under it. SPhP rays propagating from their point of excitation to the probe with a reflection (shown as black arrows) would significantly complicate the calculations.

\*Also at HSE University, Moscow, Russia 101000.; Electronic address: kaza@itep.ru

in excitation and propagation of the SPhP electromagnetic field, except for a rather thin (100-900nm) layer [9]. Nevertheless some observed wave patterns on metallized *SiC* surface were explained by the generation of the surface wave by the metal mask edge [12].

Our paper experimentally demonstrates an important yet not evident fact: the absence of phonon-polariton wave reflection at the edge of a metallic mask on the *SiC* surface using SNOM methods. This feature makes polaritonics at nearly-resonant surfaces of polar crystals different from that in thin layers and heterostructures. If the reflection of SPhP waves from the edge took place in *SiC*, then the calculation of the field configuration in the structures, with subsequent modeling and prediction of the properties, would be a very difficult task. The absence of reflection from the metal mask allows us to simplify the calculations within the semi-analytical Green-function-based method, that is crucial for modeling SPhP devices.

**Experimental methods.** The surface electromagnetic wave field is investigated using a scattering-type apertureless scanning near-field optical microscope (sSNOM) [17, 18] (see fig.1) under normal conditions. Metallized *MFG01-Pt* probes with a mechanical resonance frequency of 55 – 60 kHz were used; the amplitude of oscillations of the tip height above the sample was 50-70 nm. The signal beam of the Michelson scheme was focused by an objective onto the probing tip and onto the *SiC* sample around it. The focal spot size was about 50–80 $\mu$ m around the tip at a wavelength of  $\lambda \sim 10.7\mu$ m. The spatial resolution of sSNOM is determined by the radius of the probe tip (below 30 nm). The signal extracted by sSNOM during optical homodyning [18–20], with its amplitude and phase, is proportional to the complex amplitude of the local electromagnetic field  $E_{loc}(x, y)$  at the point of the tip location  $(x, y)$ , as found for SPhP waves on the surface of *SiC* [8, 21, 22].

**Theoretical background.** It was previously suggested [21, 23] that in some simple cases, the running and standing polariton waves excited by incident light on the *SiC* surface can be described by integrating the Green's function, similar to plasmonics [24, 25]. Within this approach, amplitude of the laser field under the metal mask is zero, whereas uncovered areas are sources of diverging SPhP waves, with the amplitude and phase determined by the amplitude and phase of the external laser field  $E_{las}(x', y')$ , where  $(x', y')$  are coordinates. All such waves propagate along the surface to the observation point  $(x, y)$ , where the probing tip is located. Thus, the probing tip dipole is driven by a local field  $E_{loc}(x, y) = E_{las}(x, y) + E_{SPhP}(x, y)$ . The second term in this expression can be expressed as an integral

$$E_{SPhP}(x, y) = \xi \int_{SiC} E_{las}(x', y') G(\Delta r_{xy}) dx' dy', \quad (1)$$

where the index *SiC* implies the integration over the open *SiC* surface from which the polariton wave can propagate

to the probe tip along a straight line. The Green's function is denoted as  $G()$ , and its argument  $\Delta r_{xy}$  means the distance from each elementary source  $(x', y')$  to the tip  $(x, y)$ . The complex Green's function is the Hankel function  $H_0(k_{xy}(\omega)\Delta r_{xy})$ , with an argument corresponding to the eigenvalue  $k_{xy}(\omega)$  found by solving the homogeneous wave equations for a surface polariton [4–7]:

$$k_{xy}(\omega) = \frac{\omega}{c} \sqrt{\frac{\varepsilon_{ab}\varepsilon_{bn}(\omega)}{\varepsilon_{ab} + \varepsilon_{bn}(\omega)}} \quad (2)$$

The indices *ab* and *bn* denote the dielectric constant of the medium above and below the interface, respectively. Above the interface, a vacuum is usually assumed ( $\varepsilon_{vac} \equiv 1$ ). Below the interface, a polar crystal is located, the analytical expression for the dielectric function of which [4–7] can be written as follows:

$$\varepsilon_{bn}(\omega) = \varepsilon_{\infty} \left( 1 + \frac{\omega_L^2 - \omega_T^2}{\omega_T^2 - \omega^2 - i\omega\Gamma} \right) \quad (3)$$

The values of  $\omega_T$ ,  $\omega_L$ , and  $\Gamma$  can be determined independently from the Raman spectra; see, e.g., [2, 26, 27]. The parameter  $\varepsilon_{\infty}$  is the dielectric function at a frequency well above the lattice vibration frequencies. The function  $H_0(k_{xy}(\omega)\Delta r_{xy})$  is a solution of the wave equation [4–7] in cylindrical coordinates, so the integral (1) must also be a solution of the wave equation.

Importantly, the SPhP waves are generated not at the metal edges, but rather over the whole metal-uncovered area [4–7]. Without the metal mask, these elementary circular waves are emitted in all directions almost isotropically, having a small total momentum. Metal-covered areas introduce asymmetry to the problem and make the momentum uncompensated.

To demonstrate the usefulness of the presented model, let us consider an example of the wave pattern formed by a small *Au* island measured similarly to Ref. [11], see fig.2. In that paper, in order to explain the observations, the oscillating dipoles excited by pumping in the gold island and then emitting SPhP waves along the surface were artificially introduced. The SNOM signal is the sum of a plane wave incident directly from the laser and polariton waves propagating along the surface. Therefore, at some points, where the phase of the wave concentrically diverging from the island and the laser wave are opposite, their sum should be equal to zero. The geometric location of such points should be a plane hyperbola. However, hyperbolic "calm" region is experimentally not observed. Another disadvantage of the dipole model is the absence of an explanation for why the amplitude of the wave launched by the dipole backwards the pump radiation is significantly smaller than the amplitude of the wave excited in the direction of the laser beam.

Calculations with the Green function straightforwardly resolve the above contradictions and allow simulations of

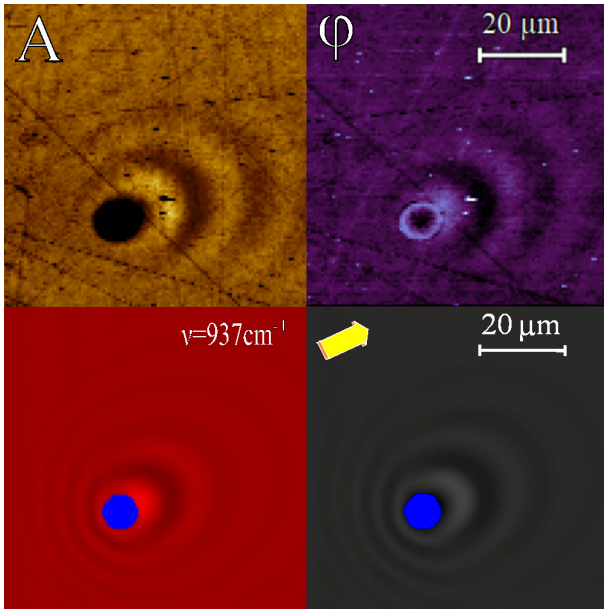


FIG. 2: Amplitude (left panels) and phase (right panels) of sSNOM signal collected (top panels) with an external irradiation near a round island of an *Au* mask (diameter  $8 \mu\text{m}$ ) on the *SiC* surface. Bottom panels show the Green-function based-simulations. Laser beam direction is shown with an arrow.

the SPhP wave patterns excited on the *SiC* surface by resonant light in the presence of a metal mask without additional assumptions. The SPhP wave field is straightforwardly obtained by integration (Eq. 1) for the known diameter of the island. The result of such a simulation is shown in Fig.2 and agrees well with the experimental data and, of course, has no hyperbolic "calm" region.

Reflections of waves from the boundaries of the golden masks at the edge of the window (black rays of polariton waves in Fig.1) and their further propagation over the *SiC* surface in the mask window make the calculations insurmountably complicated.

**Experimental result.** In this paper, we present an experimental observation and qualitative considerations in favor of the absence of noticeable reflections of the surface polariton wave from the edge of a metal mask. The straight edge of the mask in the presence of a plane light wave incident on the sample turns out to be a source of a polariton wave traveling along the surface [28], the wave front of which is also straight. In sSNOM images of this traveling wave, the phase front turns out to be parallel to the mask boundary [8, 21, 22].

If the SPhP wave were reflected from the straight edge of the metal mask on the sample surface, a series of beating fringes corresponding to the wave propagating in a new direction should appear. We formed (Fig.3) the following structure on the surface of the *SiC* sample: two straight edges of the metal (*Au*, 50 nm) mask, between which there is an acute corner of the *SiC* surface open to irradiation. In the experiment, two series of

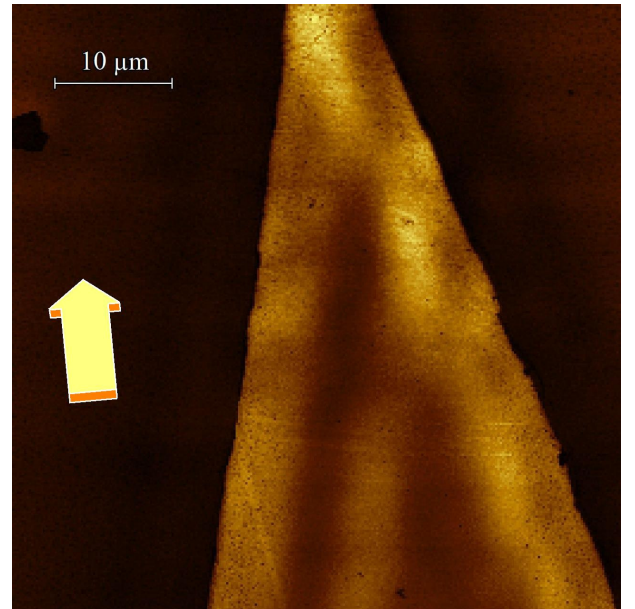


FIG. 3: Image of the amplitude of the sSNOM signal obtained on an open, acute-angled region of the *SiC* surface, on which the incident (in the direction shown by the arrow) light wave excites running phonon-polariton waves. The  $\text{CO}_2$  laser line used ( $\nu = 935 \text{ cm}^{-1}$ ). Waves with phase fronts parallel to the source edge are visible. Waves with phase front directions corresponding to geometric reflection are absent.

beating fringes are observed between the laser beam field  $E_{las}(x, y)$  and the fields  $E_{SPhP}^{(1)}(x, y)$  and  $E_{SPhP}^{(2)}(x, y)$  of polariton waves launched from the two straight edges of the gold mask. The reflection of a wave, initially launched by one edge, from the opposite edge of the triangular *SiC* "bay" should have a third direction, not coinciding with either of the two listed. No such wave is observed, indicating the absence of reflection.

**Discussion.** Another, indirect experimental indication of the absence of a noticeable reflection of the phonon-polariton wave running along the *SiC* surface from the boundary of the polariton-active area is given by a comparison with systems in which such a reflection does exist. For example, in sSNOM images of nanometer-thick samples near the boundary of a film of polariton-active substances (graphene [14], boron nitride [15],  $\text{MoS}_2$  [16], germanium [10]), there is a series of parallel fringes with a period that weakly depends on the orientation of the film edge with respect to the direction of the exciting light. Such a wave pattern corresponds to a surface polariton wave, which was launched by the probing tip and then reflected from the edge of the polariton-active film. After reflection from the straight line of the boundary, this polariton wave diverging from the "image" tip returned back to the probe and modified the tip's electromagnetic response with its field, changing the parameters of the light wave emitted by the probe into space. The observed series of interference fringes of the probing tip field with its own reflection at the edge of the film quickly fades

away with distance from the edge of the film, since the diverging concentric wave is described by the cylindrical Hankel function (its amplitude decreases approximately inversely proportional to the distance from the source), and, thus, the amplitude of the field of the wave received from the mirror image of the tip at the boundary of the film should decrease according to the same law. A similar series of rapidly decaying waves near the edge of the metal mask was not observed in experiments on the *SiC* surface [8, 11–13, 21, 22].

It is important to highlight the difference between light-excited plasmon-polariton in metal structures on dielectric substrate (for example [28–30]) and SPhP wave on the metallized *SiC*. For plasmon polariton the edge of the polariton-active medium (metal film) turns out to be spatially sharp for the entire depth of the film. Therefore surface wave reflection is effective and integration of the Green function does not bring satisfactory description. This is opposite to the SPhP case described in this paper. We would also expect high reflection of the SPhP waves from the boundary of a 100 nm-thick *SiC* film mentioned in [9]. Such a thickness is significantly less than an SPhP wave penetration depth in *SiC*, so that the electromagnetic boundary of the slab happens at the same edge line for the whole depth.

Let us consider theoretical arguments in favor of the absence of noticeable reflection of the SPhP wave on the *SiC* surface from the edge of the metal mask. The depth of exponential decay of the field in the  $z$ -direction, perpendicular to the surface, is estimated as follows [4–7]:

$$\delta_{z(bn)}(\omega) = \frac{\omega}{c} \frac{\varepsilon_{bn}(\omega)}{\sqrt{\varepsilon_{bn}(\omega) + \varepsilon_{ab}}} \quad (4)$$

When substituting into (4) the expression (3), this depth is, depending on the frequency, from  $0.06\lambda = 70\text{nm}$  at the lattice resonance frequency  $\nu_T = 795\text{cm}^{-1}$  to  $0.5\lambda = 6\mu\text{m}$  near the frequency of the edge of the polariton state band, approximately equal to  $\nu_L = 961\text{cm}^{-1}$  [3]. The appearance of a sharp edge of the mask over the polariton wave along the surface does not immediately have a strong influence on it, because the vast majority of electromagnetic energy is concentrated in crystal at a depth of up to  $5\mu\text{m}$ . In three-dimensional (optics) and one-dimensional (cable) wave processes, effective reflection of a wave from the boundary of a medium occurs in cases where the spatial scale of the step in permittivity, or wave resistance, is smaller than the wavelength. In optics, such a case is described by the Fresnel formulas. The reflection coefficient of a radio signal from a broken or short-circuited end of a cable is also easily calculated using the known impedance of the short circuit at a point. In the case where the wave properties change "adiabatically smoothly" over a segment comparable to or greater than the wavelength, the wave reflection weakens or disappears completely.

The propagation length of the polariton wave under the gold mask can be estimated by substituting the upper medium  $\varepsilon_{ab}(\omega)$  material parameters for the gold film

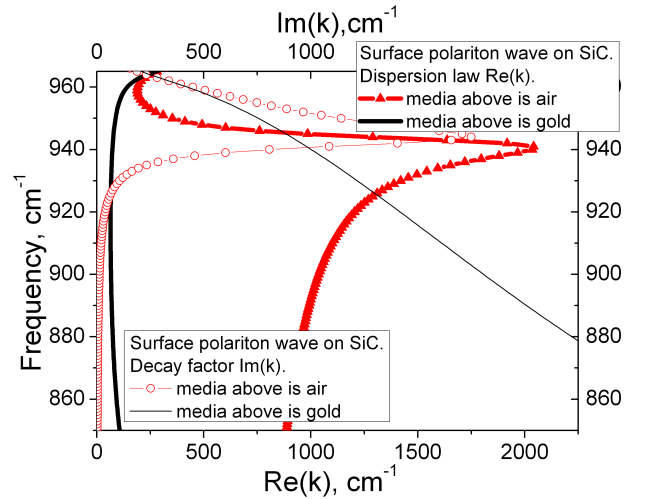


FIG. 4: Dependence of the real (bold lines) and imaginary (thin lines) parts of the wave vector (horizontal scale) on the frequency (vertical scale) for phonon-polariton waves on the surface of *SiC* under vacuum (red curves) and under gold (black curves).

[31] into the expression (2). This approach is consistent with the logic of classical works on the theory of phonon-polariton waves [4–7] and does not contradict any general assumptions. Fig.4 shows the result of the calculations.

It can be seen in the figure 4, that (a) the phase velocity of the polariton wave under gold is very high (i.e., that the polariton oscillations in the "wave" that has penetrated under the gold layer have the same phase everywhere), and (b) the wave decay length is comparable to the wavelength over the open surface of *SiC*.

**Conclusion.** In this work, it has been experimentally shown that the reflection of phonon-polariton waves running on the *SiC* surface from the boundaries of the metal mask can be neglected. The polariton waves, once excited by irradiating light on the surface, disappear, getting under the edge of the mask. The first indirect indications in favor of absence of reflections were repeatedly reproducible agreements of the experimentally observed wavefields with a Green function-based wavefront calculation for the metallized masks of very complex shape on the *SiC* surface under resonant irradiation [8, 13, 21]. In this paper we suggested an experiment-crucious with a wedge-shaped mask and did not detect polariton waves launched by one straight edge of the mask and then reflected by the other one. This property of the polar crystal surface radically differs from that of metal films used as carriers of plasmon-polariton waves in the visible region of the spectrum, as well as from nanometer graphene films and VdW crystals studied in the infrared region of the spectrum. Due to this property, the configuration of standing and running phonon-polariton waves excited by an incident external coherent light wave in the presence of a metal screening mask of an arbitrary configuration can be calculated by integrating the Green's function.

**Acknowledgements** The sample fabrication was performed at the Shared Facility center at the P.N. Lebedev

Physical Institute.

- 
- [1] D. N. Basov, A. Asenjo-Garcia, P. J. Schuck, X. Zhu, and A. Rubio, *Nanophotonics* **10**, 449 (2021), URL <https://www.degruyter.com/document/doi/10.1515/nanoph-2020-0449/html>.
- [2] Y. Sasaki, Y. Nishina, M. Sato, and K. Okamura, *Phys. Rev. B* **40**, 1762 (1989), URL <https://link.aps.org/doi/10.1103/PhysRevB.40.1762>.
- [3] D. Bimberg, R. Blachnik, P. Dean, T. Grave, G. Harbeke, K. Hübner, U. Kaufmann, W. Kress, O. Madelung, et al., *Physics of Group IV Elements and III-V Compounds / Physik Der Elemente Der IV. Gruppe und Der III-V Verbindungen*, Landolt-Bornstein: Numerical Data and Functional Relationships (Springer, 1981), ISBN 9783540106104, URL <http://books.google.de/books?id=6Ar7741aEywC>.
- [4] R. H. Lyddane, R. G. Sachs, and E. Teller, *Phys. Rev.* **59**, 673 (1941).
- [5] T. H. K. Barron, *Phys. Rev.* **123**, 1995 (1961), URL <https://link.aps.org/doi/10.1103/PhysRev.123.1995>.
- [6] R. Ruppin and R. Englman, *Rep. Prog. Phys* **33**, 149 (1970).
- [7] D. L. Mills and E. Burstein, *Reports on Progress in Physics* **37**, 817 (1974), URL <http://iopscience.iop.org/0034-4885/37/7/001/>.
- [8] A. Huber, N. Ocelic, D. Kazantsev, and R. Hillenbrand, *Applied Physics Letters* **87**, 081103 (pages 3) (2005), URL <https://pubs.aip.org/aip/apl/article/87/8/081103/117557/Near-field-imaging-of-mid-infrared-surface-phonon>.
- [9] A. Mancini, L. Nan, F. Wendisch, R. Berté, H. Ren, E. Cortés, and S. Maier, *ACS Photonics* **9**, 3696 (2022), URL <https://doi.org/10.1021/acsp Photonics.2c01270>.
- [10] A. M. Dubrovkin, B. Qiang, T. Salim, D. Nam, N. I. Zheludev, and Q. J. Wang, *Nature Communications* **11**, 1863 (2020), ISSN 2041-1723, URL <https://doi.org/10.1038/s41467-020-15767-y>.
- [11] A. Huber, N. Ocelic, and R. Hillenbrand, *Journal of Microscopy* **229**, 389 (2008), URL <http://dx.doi.org/10.1111/j.1365-2818.2008.01917.x>.
- [12] A. J. Huber, B. Deutsch, L. Novotny, and R. Hillenbrand, *Applied Physics Letters* **92**, 203104 (pages 3) (2008), URL <http://link.aip.org/link/?APL/92/203104/1>.
- [13] V. S. Ivchenko, D. V. Kazantsev, V. A. Ievleva, E. A. Kazantseva, and A. Y. Kuntsevich, *Applied Physics Letters* **125**, 171601 (2024), ISSN 0003-6951, <https://pubs.aip.org/aip/apl/article-pdf/doi/10.1063/5.0229574/20219776/171601.1.5.0229574.pdf>, URL <https://doi.org/10.1063/5.0229574>.
- [14] J. Chen, M. Badioli, P. Alonso-Gonzalez, S. Thongrattanasiri, F. H. J. O. M. S. A. Centeno, A. Pesquera, P. Godignon, A. Z. Elorza, N. Camara, F. J. G. de Abajo, et al., *Nature Letters* **487**, 77 (2012), URL <http://dx.doi.org/10.1038/nature11254>.
- [15] S. Dai, Q. Ma, M. K. Liu, T. Andersen, Z. Fei, M. D. Goldflam, M. Wagner, K. Watanabe, T. Taniguchi, M. Thiemens, et al., *Nature Nanotechnology* **10**, 682 (2015), ISSN 1748-3395, URL <https://doi.org/10.1038/nnano.2015.131>.
- [16] A. M. Dubrovkin, B. Qiang, H. N. S. Krishnamoorthy, N. I. Zheludev, and Q. J. Wang, *Nature Communications* **9**, 1762 (2018), ISSN 2041-1723, URL <https://doi.org/10.1038/s41467-018-04168-x>.
- [17] H. Wickramasinghe and C. Williams, *Apertureless near field optical microscope* (1990), uS Patent 4,947,034, URL <http://www.google.com/patents/US4947034>.
- [18] F. Zenhausern, M. P. O'Boyle, and H. K. Wickramasinghe, *Applied Physics Letters* **65**, 1623 (1994), URL <http://link.aip.org/link/?APL/65/1623/1>.
- [19] M. Labardi, S. Patanè, and M. Allegrini, *Applied Physics Letters* **77**, 621 (2000), URL <http://link.aip.org/link/?APL/77/621/1>.
- [20] F. Keilmann and R. Hillenbrand, *Philosophical Transactions: Mathematical, Physical and Engineering Sciences* **362**, 787 (2004), ISSN 1364503X, URL <http://www.jstor.org/stable/4142390>.
- [21] D. V. Kazantsev, *JETP Letters* **83**, 323 (2006), URL <http://link.springer.com/article/10.1134/S0021364006080054>.
- [22] D. Kazantsev and H. Ryssel, *Applied Physics A* **113**, 27 (2013), URL <http://dx.doi.org/10.1007/s00339-013-7869-y>.
- [23] D. V. Kazantsev and E. A. Kazantseva, *JETP Letters* **107**, 512 (2018), ISSN 1090-6487, URL <https://doi.org/10.1134/S0021364018080106>.
- [24] A. V. Zayats, I. I. Smolyaninov, and A. A. Maradudin, *Physics Reports* **408**, 131 (????), URL <https://www.sciencedirect.com/science/article/abs/pii/S0370157304004600>.
- [25] J. R. Krenn, A. Dereux, J. C. Weeber, E. Bourillot, Y. Lacroute, J. P. Goudonnet, G. Schider, W. Gotschy, A. Leitner, F. R. Aussenegg, et al., *Phys. Rev. Lett.* **82**, 2590 (1999), URL <https://link.aps.org/doi/10.1103/PhysRevLett.82.2590>.
- [26] D. W. Feldman, J. H. Parker, W. J. Choyke, and L. Patrick, *Phys. Rev.* **170**, 698 (1968), URL <https://link.aps.org/doi/10.1103/PhysRev.170.698>.
- [27] H. Harima, S. Nakashima, and T. Uemura, *Journal of Applied Physics* **78**, 1996 (1995), URL <http://link.aip.org/link/?JAP/78/1996/1>.
- [28] Y. J. Chabal and A. J. Sievers, *Applied Physics Letters* **32**, 90 (1978), ISSN 0003-6951, <https://pubs.aip.org/aip/apl/article-pdf/32/2/90/7739702/90.1.online.pdf>, URL <https://doi.org/10.1063/1.89947>.
- [29] T. Atay, J.-H. Song, and A. V. Nurmikko, *Nano Lett.* **4**, 1627 (2004), ISSN 1530-6984, URL <https://doi.org/10.1021/nl1049215n>.
- [30] O. L. Muskens, V. Giannini, J. A. Sánchez-Gil, and J. G. Rivas, *Opt. Express* **15**, 17736 (2007), URL <https://opg.optica.org/oe/abstract.cfm?URI=oe-15-26-17736>.
- [31] M. A. Ordal, R. J. Bell, R. W. Alexander, L. L. Long, and

M. R. Query, Appl. Opt. **24**, 4493 (1985), URL <http://ao.osa.org/abstract.cfm?URI=ao-24-24-4493>.